

Investigation of the mouse visual pathway via high-field functional MRI

Francisca Faria Fernandes
francisca.fernandes@tecnico.ulisboa.pt

Thesis to obtain the Master of Science Degree in Biomedical Engineering
Supervisors: Dr. Noam Shemesh and Prof. Patrícia Margarida Piedade Figueiredo

Instituto Superior Técnico, Lisboa, Portugal
November 2017

Abstract

The visual system is highly complex and distributed throughout the brain. Many methods, such as electrophysiological recordings and EEG, have provided immense insight into the visual pathway's underpinnings; however, capturing the entire distributed pathway in rodents – and in particular in the versatile mouse models *vis-à-vis* transgenesis and optogenetics – would be represent a major step forward. Functional MRI (fMRI) can non-invasively investigate the underpinnings of the visual system, but most studies in mice to date relied on presentation of simple flickering stimuli. Moreover, current anaesthesia approaches aimed at avoiding animal motion are ineffective in some strains of mice and incompatible with long scanning times required for delivery of more complex stimuli. Here, we present the development of a visual stimulation system capable of delivering diversely shaped polychromatic stimuli through a 96x64 matrix in the scanner. We further developed a novel anaesthetic protocol based on subcutaneous infusion of etomidate – a sedative allowing much more stable anaesthesia while preserving Blood-Oxygenation-Level-Dependent (BOLD) contrasts – and tested it for the first time in rodent fMRI through three complementary experiments. Significant BOLD responses were recorded along the visual pathway following binocular stimulation. A clear dependence on the frequency and intensity of flashing lights was demonstrated. The suitability of this anaesthetics for future functional studies has been confirmed, and bench tests suggested that significantly smaller doses can be used in the future, thereby providing further experimental stability and flexibility. All these facilitate the study of complex visual stimuli with BOLD fMRI.

Keywords: fMRI, Visual Stimulation, Etomidate, Mouse model

1. Introduction

Many animals, as well as humans, rely on vision as their dominant sense to evaluate their surroundings and guide their behaviour. Understanding how the brain gives rise to the experience of sight has been the focus of much attention over the years, especially in Neuroscience, but also in many biomedical studies.

The mouse visual system is becoming a predominant model for investigating underlying disease mechanisms and experience-dependent plasticity, including in the visual pathway [1], mainly since mice provide excellent genetic flexibility, which enables unique experimental settings such as optogenetic control of specific neurons or models of disease [2].

The visual pathway is widespread in the brain. Optic nerves exit from the retinas and decussate at the chiasm. The fibres then enter the optic

tract, which projects to three main subcortical regions: the lateral geniculate nucleus (LGN), which is an important relay centre involved in visual perception; the superior colliculus (SC), known to mediate visual reflexes [3], orienting head and body movements [4] and initiating defensive behaviours [5]; and the pretectum, associated with the production of pupillary reflexes. The primary visual cortex (V1) is the terminal station of the optic radiation from the dorsal LGN and represents an important area for processing of a wide variety of complex stimuli.

Most studies on the mouse visual system were conducted with invasive and small field of view (FOV) techniques [6][7][8]. However, a complementary approach involves methods capable of capturing activity along the entire pathway. Functional magnetic resonance imaging (fMRI) based on the Blood Oxygenation Level Dependent (BOLD) contrast provides information on activity with very good spatial resolution and extensive

brain coverage [9]. fMRI's non-invasive nature also makes it optimal for longitudinal experiments. In monkeys and humans, fMRI has been vastly employed to study the visual system [10][11][12]; however, in rodents, visual stimuli are scarcely used in the context of fMRI, and setups for visual presentation are nearly always limited to simple flickering stimuli [13][14].

A related issue with the paucity of mouse fMRI experiments is the proper choice of the anaesthetic regime. fMRI-compatible anaesthetics commonly used for fMRI in mice, such as medetomidine, have several drawbacks. Particularly, medetomidine's action proved ineffective in numerous mouse lines [15] and the sedative effects of medetomidine often do not last for more than 1-2 hours, after which animal motion typically occurs. More complex fMRI experiments that require longer scanning periods are thus compromised. To overcome the shortcomings of this and other similar agents, a novel anaesthesia regime for small animal imaging based on i.v. infusion of etomidate has been proposed and tested [15]. Etomidate provided long-term stable physiological conditions, preserved neurovascular coupling and afforded full recovery from anaesthesia in spontaneously breathing animals. However, this protocol requires intravenous administration, which carries risks of fluid overload and pulmonary edema [16]. Although a much simpler protocol for subcutaneous delivery has already been reported [17], its applicability for fMRI in the mouse remains to be verified.

In this study, we aimed to develop a system for preclinical fMRI of the mouse visual pathway, that would enable the delivery of accurate and complex stimuli (e.g. moving, projection of different shapes, polychromatic, etc.). As a crucial step, we also developed a mice anaesthesia protocol involving subcutaneous etomidate. BOLD response dynamics following flickering visual stimuli of different light intensities and frequencies were tested, with promising results towards application in the more complex setup.

2. Materials and Methods

All aspects of these study were preapproved by the Champalimaud Centre for the Unknown's Ethics Committee operating under Portuguese and EU Law.

2.1. Visual Stimulation fMRI Experiments

Three different experiments were performed to investigate the applicability of subcutaneous etomidate on BOLD fMRI in the mouse: two investigated the BOLD response of etomidate-sedated mice to different (1) light intensities and (2) frequencies, while (3) the other provided

comparative data of medetomidine-sedated mice to these experiments.

Animal Preparation. A total of 11 male C57BL6/J mice aged between 7 to 8 weeks old were used: n=4 for Experiment 1 (20 to 27 g), n=4 for Experiment 2 (24 to 27 g), and n=3 for Experiment 3 (24 to 27 g). Anaesthesia was induced with a mixture of 5% isoflurane and ambient air, which was decreased to 3% during preparation, and maintained with etomidate (23 mg/kg bolus, 0.6 mg/kg/min initiated 5-10 minutes after bolus) for Experiments 1 and 2 and with medetomidine (0.4 mg/kg bolus, 0.8 mg/kg/h infusion initiated 10 minutes after bolus) for Experiment 3, similar to the protocols suggested by Klee et al. [17] and Adamczak et al. [18], respectively. Temperature and respiration sensors were placed for real-time monitoring of mouse physiology. A heated water bed was used to avoid body temperature to drop dramatically after induction of anaesthesia and eye drops were applied in both eyes to prevent drying of the corneas. At the end of Experiment 3, a subcutaneous injection of atipamezole at 2 mg/kg was administered to recover the mice.

Visual Stimulation System. A LED with central wavelength located at 470 nm (blue) was coupled to an ~8 m two-branching fibre-optic patch cord to conduct light to the magnet bore in a MRI-compatible fashion and allow binocular stimulation. Zirconia sleeves were then connected to each of the two fibre-optic patch cord ends to diffuse light, rendering it less aggressive to the eyes. 3-D pieces were designed and printed for stable and accurate positioning of the fibres across experiments. Synchronization with the MRI scanner and accurate control of stimulus presentation were accomplished through an Arduino Mega for trigger detection and LED driver control.

MRI protocol. Experiments were carried out on a 9.4T horizontal MRI scanner equipped with a gradient system capable of producing up to 660 mT/m in all directions. An 86 mm inner diameter quadrature resonator was used for RF transmission and a 10 mm inner diameter loop surface coil was used for signal reception. Once the animal was properly positioned in the scanner, the magnet bore was covered to prevent the entrance of external light. Scout images were acquired in three orthogonal planes with a Fast Low Angle Shot (FLASH) pulse sequence (TR = 50 ms, TE = 3.5 ms, flip angle = 20°, matrix size = 160 x 160, FOV = 16 x 16 mm², slice thickness = 0.6 mm) in order to assess the quality of position of the head in 3-D. A B_0 field map was then obtained and field inhomogeneities were corrected through shimming. High-resolution anatomical images were acquired using a Rapid Acquisition with Relaxation Enhancement (RARE) sequence

with: RARE factor = 8, number of averages = 4, TR = 2000 ms, TE = 8.8 ms, matrix size = 200 x 160, FOV = 20 x 16 mm², and 20 parallel 0.6 mm thick coronal slices, such that the fourth slice was approximately centred in the transverse fissure of the brain. fMRI data were then acquired using a Gradient-echo Echo-planar imaging (GE-EPI) sequence with: TR = 1000 ms, TE = 15 ms, matrix size = 120 x 84, FOV = 17 x 12 mm² (yielding, therefore, an in-plane resolution of 142 x 143 μm²), flip angle = 55°, and 13 parallel coronal slices each 0.5 mm thick, separated by gaps of 0.1 mm, such that the first slice was approximately centred in the transverse fissure of the brain. Slice acquisition order was interleaved with the order being: [1 3 5 7 9 11 13 2 4 6 8 10 12].

Visual Stimulation Paradigm. The stimulus was delivered using a block-design paradigm of alternating 40 s rest and 20 s activation repeated 5 times. In Experiment 1, two different stimulation frequencies (2 Hz and 10 Hz) and three different light intensities (9.2×10^{-3} W/m², 9.2×10^{-2} W/m² and 8.1×10^{-1} W/m²) were chosen based on previous studies of visual stimulation responses in the rodent brain [14][19], resulting in 6 different stimulation conditions. The duration of the stimulation pulses was always 10 ms. Each fMRI scan was conducted twice for each condition, resulting in 12 runs per mouse. Mice were allowed to rest 7-10 minutes between runs. In Experiment 2, the duration and intensity of the flickering pulses were kept constant at 10 ms and at 8.1×10^{-1} W/m², respectively. Stimulation frequencies, on the other hand, were varied between 2 Hz, 5 Hz, 10 Hz and 20 Hz. Each condition was again repeated twice for each mouse, resulting in a total of 8 runs per mouse. Moreover, the mice were allowed to rest for 7 minutes before the beginning of another run. In Experiment 3, only one condition was tested: the LEDs were flashed at a frequency of 2 Hz and a pulse width of 10 ms, and light intensity reaching the eyes was fixed at 8.1×10^{-1} W/m². Between 5-9 runs were completed for each mouse in every session, depending on the animal's physiological stability, with intervals of 8 minutes between each run.

fMRI data analysis. All data was analysed using the SPM12 package and some user-defined functions and routines in Matlab. The ImageJ software [20] was also used to draw ROIs for the ROI analyses. Functional images' SNR was calculated and averaged over all animals. The average signal timecourse in each brain slice was then plotted for detection of signal fluctuations in the data. In addition, the signal from each voxel in the brain slice was displayed in a 2-D map in order to also help detecting those outliers in the data. After manual selection of those time points, the intensity of the voxels in the non-masked

slice at those time instants was replaced by doing a cubic spline interpolation from the signal those voxels had in the remaining time points. Images from each functional run were then corrected for slice-timing differences, realigned to the mean volume, coregistered to the anatomical volume and normalized to the Allen mouse brain atlas (2012 version) [21]. Finally, fMRI data was spatially smoothed using a 3D Gaussian kernel with a full width at half maximum (FWHM) of 0.28 mm. For statistical parametric mapping, a 1st level general linear model (GLM) analysis was conducted for each functional run and for each subject under each condition. All subject scans for each condition were also included in a single GLM in order to build global maps of activation for each condition. In either case, a double gamma-function peaking at 1.40 s after stimulus onset was used to model the HRF, and the six realignment parameters were used as nuisance regressors. The default SPM12 options of grand mean scaling and auto-correlation modelling were also used, with a high-pass filter of 80 s to remove slow signal drifts. The parameters of the GLM were estimated and positive and negative contrasts were defined. A *t*-test was then performed for both contrasts on a voxel by voxel basis and thresholds for significance applied. ROIs were drawn around the SC, the LGN and the V1 on the reference brain according to the Paxinos and Franklin's mouse brain atlas [22]. These masks were then applied to the normalized unsmoothed images and the average time series from all enclosed voxels was computed. Thereafter, each timecourse was detrended, normalized to percentage signal change, and averaged over stimulus blocks for each run so that a representative cycle could be shown. Both the timecourses and the average cycles were then averaged across runs and mice and the BOLD peak amplitude of the average cycles was registered.

2.2. Optimization of Etomidate Dosage

Bench tests were performed to understand if it was possible to decrease the dosage of etomidate and thus decrease the mortality rate that comes from it, while maintaining a constant depth of anaesthesia for three hours. 9 male C57BL6/J mice aged between 7 to 8 weeks old were administered a bolus and constant infusion of etomidate at 23 mg/kg and 0.6 mg/kg/min, respectively. After 35 min of bolus, mice were divided into 3 groups: group 1 continued to be administered 0.6 mg/kg/min, while group 2 and group 3 started to be administered 0.3 mg/kg/min and 0.2 mg/kg/min, respectively. Furthermore, discontinuation of isoflurane was extended in time to avoid movements after isoflurane was lowered to 0%.

2.3. Setup for Delivery of Complex Visual Stimuli

The novel visual stimulation setup was built using a 0.95-inch OLED display module with a 96 x 64 dots matrix and 16-bit color depth. The screen was connected through a 1.5 m cable to its breakout module. The cable was properly isolated with layers of a fine metal mesh so that the OLED circuitry did not suffer from induced currents from gradients field, avoiding therefore any interference on image acquisition or contamination of the visual patterns presented by the OLED. The synchronization with the MRI scanner protocol and accurate control of the stimulus presentation was accomplished through an Arduino Due microcontroller for trigger detection and OLED control. A 3-D piece was also designed and printed to guarantee that the screen would always be placed in the same position across experiments, i.e. at approximately 2.5 cm from the left eye, and that the optical axis of the mouse intercepted the screen in the middle of the field of view to be used (a 64 x 64 pixel square region in the right part of the screen). Each pixel spans less than 0.5° of the visual field in each direction, and the total FOV covers ~30° x 30° of the visual field. The entire system with all of its components assembled together is shown in Figure 1.

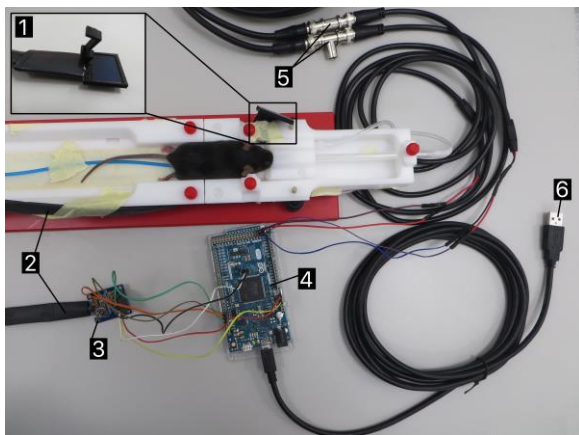


Figure 1 – Experimental setup for visual pathway mapping in the mouse, with all the elements that are essential for the delivery of complex visual stimuli. (1) OLED display inserted in the 3-D modelled piece that attaches to the bed, (2) 1.5 m cable that is used to put all electronic components away from the inside of the scanner bore, (3) OLED breakout module, (4) Arduino Due microcontroller, (5) Cables and connectors used to allow the reception of 2 TTL trigger signals from the scanner. A tee connector is used in one of these two connections to also allow the physiological monitoring gating system to record when fMRI data acquisition is occurring, (6) Cable that connects the Arduino to the computer.

The OLED was programmed to present moving bars of different speeds along the temporal-nasal and upward-downward directions to the left eye of the mouse, as exemplified in Figure 2. The Arduino was coded to receive two different TTL

signals from the scanner: one to trigger rest periods, in which a static vertical or horizontal bar in the OLED is kept on as long as the trigger is being received, and another to trigger stimulation periods, i.e. periods of motion of the bar. Different speeds can be produced by changing bar on-off intervals.

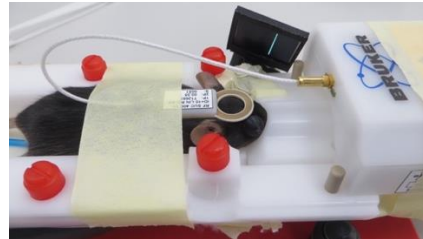


Figure 2 – Visual stimulation of the left eye with a vertical bar moving across the screen. A loop surface coil is placed above the head for RF signal reception and is connected to its pre-amplifier.

3. Results

3.1. Visual Stimulation fMRI Experiments

EPI sequences in this study performed quite well. Figure 3 shows representative images of raw fMRI data, and demonstrates relatively high SNR and relatively few distortions for an EPI sequence at 9.4T. A few cortical regions evidence signal losses in these images (white arrows) due to susceptibility effects, and slightly higher signals were observed in the dorsal parts of the brain in comparison to the lower regions due to the larger distance from the ventral regions to the loop coil used for signal reception. Nevertheless, raw functional data were reliable and robust across runs and animals, showing a high and reproducible SNR of 35.6 ± 6.2 (mean \pm standard deviation), even at the high spatial and temporal resolution they were acquired with.

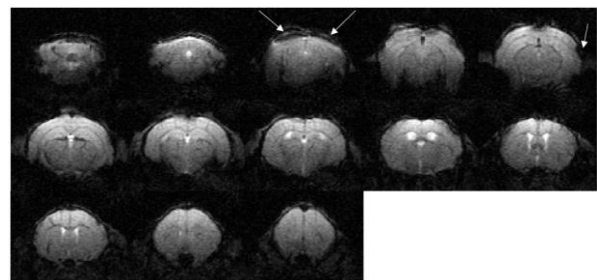


Figure 3 – Raw functional images (from one frame on a single run) from one representative mouse. Slices are presented from the caudal part to the rostral part of the brain (from left to right and top to bottom in the figure).

Clear BOLD responses were observed in ROIs placed in relevant regions along the visual pathway with the naked eye in single runs, even before averaging on the multiple runs or on different animals. After averaging all BOLD signal timecourses for identical stimulus conditions across animals, BOLD responses became easier

to detect in all ROIs following stimulation, as exemplified in Figure 4.

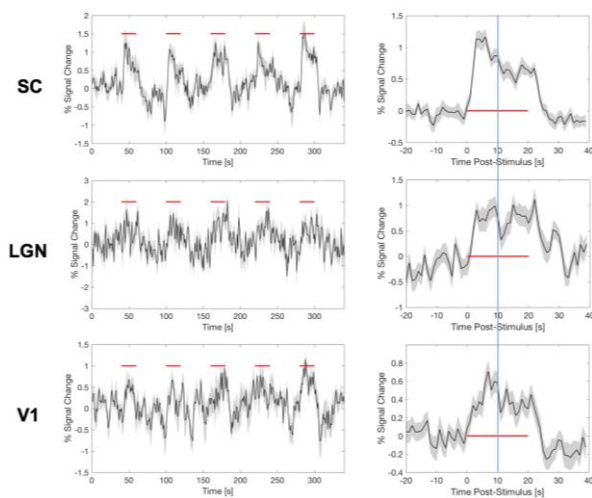


Figure 4 – BOLD responses to binocular visual stimulation with 2 Hz flashing frequency and $9.2 \times 10^{-2} \text{ W/m}^2$ of light intensity in the SC, LGN and V1, averaged over 3 animals ($n = 6$ runs) and plotted as mean percentage of signal change (solid line) \pm standard error of the mean (shaded region). Plots on the left represent mean BOLD timecourse over five stimulus epochs, while each plot on the right represents the average cycle of the BOLD response computed from the corresponding mean run on the left. The red bars indicate 20 s stimulation periods. A vertical line is drawn in the average cycle plots to guide the eye at 10 s from the beginning of stimulation.

Structures activated in individual BOLD response maps include the SC, V1 and LGN of the brain. However, small clusters of activation are also frequently found in other brain regions that are not known to be functionally related to the visual pathway. Therefore, group-level brain maps were built to find which voxels show the most significant activation across experiments. Figure 5 shows a group-level map obtained for one stimulus condition. Clusters of activation are observed in the SC, LGN and V1 with high statistical significance. However, voxels in brain regions not associated with vision that appeared active in some single subject maps were eliminated in the group analysis.

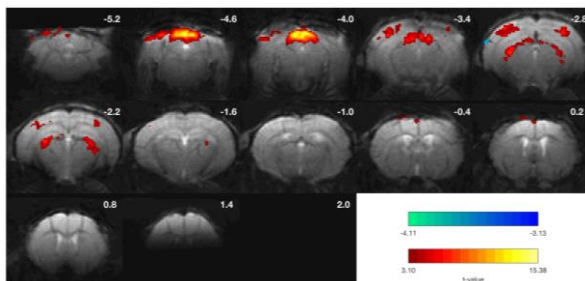


Figure 5 – Brain map of significant ($p < 0.001$, minimum cluster size = 8) BOLD activation to binocular visual stimulation with 2 Hz flashing frequency and $9.2 \times 10^{-2} \text{ W/m}^2$ of light intensity in consecutive coronal slices from an average of 3 mice ($n = 6$ runs). Approximate distances from Bregma are indicated in each slice. The most rostral image slices are cut as a result of realignment, coregistration and normalization.

Experiment 1: BOLD responses to different light intensities under etomidate

Although the physiological parameters of all mice used in Experiment 1 were stable during the entire experimental session, with a mean \pm standard deviation of 109 ± 13 breaths/min and 34.9 ± 1.4 $^{\circ}\text{C}$ across all mice, two of the mice died within one day following the experiments. This was most probably caused by the administration of etomidate. One of these revealed almost no response to the stimuli in the visual pathway. Therefore, the data from this mouse was discarded from the group analysis. The other two mice, on the other hand, returned to their normal state within some hours after the experiment.

The group-level maps for each light intensity ($9.2 \times 10^{-3} \text{ W/m}^2$, $9.2 \times 10^{-2} \text{ W/m}^2$ and $8.1 \times 10^{-1} \text{ W/m}^2$) are shown in Figure 6 for 2 Hz of flickering frequency, and in Figure 7 for 10 Hz stimuli. Since responses are mainly concentrated in 6 slices, the other 7 slices are not shown. Bilateral BOLD responses to the stimuli were clearly observed in the SC, V1 and LGN at all intensities, though with different significance levels.

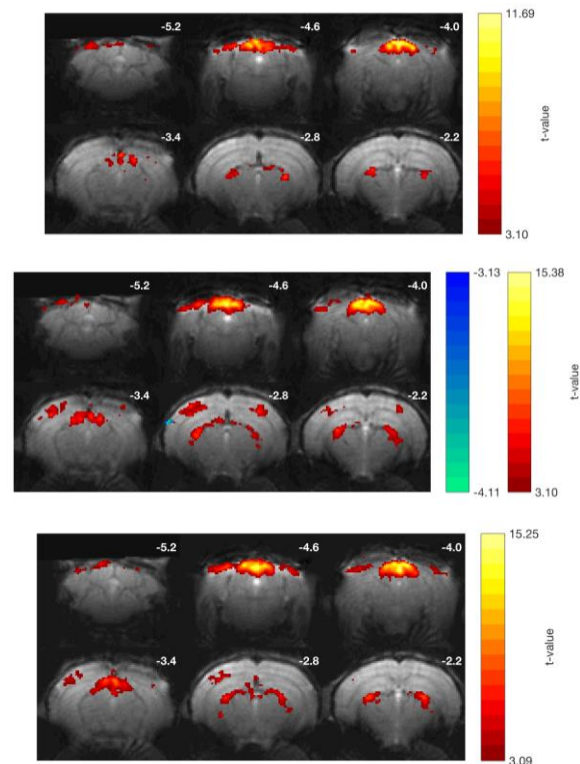


Figure 6 – Brain maps of significant ($p < 0.001$, minimum cluster size = 8) BOLD activation to binocular visual stimulation with 2 Hz flashing frequency and $9.2 \times 10^{-3} \text{ W/m}^2$ (Top), $9.2 \times 10^{-2} \text{ W/m}^2$ (Middle) or $8.1 \times 10^{-1} \text{ W/m}^2$ (Bottom) of light intensity in consecutive coronal slices from an average of 3 mice ($n = 6$ runs). Approximate distances from Bregma are indicated in each slice.

Significant SC responses are observed at all intensities for both frequencies, with the higher t -

value voxels located in the more dorsal layers. Moreover, the t -values and the number of responsive voxels appear to increase with intensity, especially at the 10 Hz flickering frequency. Similar to the SC, the size of the LGN clusters slightly increases with increasing intensity. Highly significant BOLD responses were also detected in V1 in every run for all animals. Moreover, clear bilateral negative BOLD responses were found in the cortex at 10 Hz for all intensities, while responses at 2 Hz were positive.

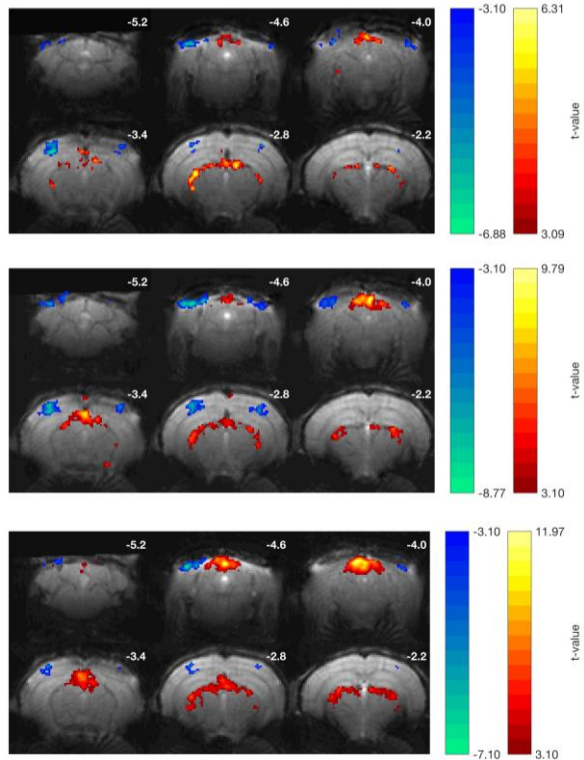


Figure 7 – Brain maps of significant ($p < 0.001$, minimum cluster size = 8) BOLD activation to binocular visual stimulation with 10 Hz flashing frequency and $9.2 \times 10^{-3} \text{ W/m}^2$ (Top), $9.2 \times 10^{-2} \text{ W/m}^2$ (Middle) or $8.1 \times 10^{-1} \text{ W/m}^2$ (Bottom) of light intensity in consecutive coronal slices from an average of 3 mice ($n = 6$ runs). Approximate distances from Bregma are indicated in each slice.

To more easily compare these results, the average BOLD response amplitudes for each stimulus condition are shown in Figure 8. Smaller peak BOLD amplitudes are detected in the SC and LGN for the lowest light intensity used ($9.2 \times 10^{-3} \text{ W/m}^2$) in comparison to the highest intensities, either for 2 Hz or 10 Hz flashing stimuli. Moreover, although a significant difference between the maximum amplitudes registered in the SC and LGN for all stimulus conditions was not observed, responses detected in V1 reach lower percent signal change values in comparison to the other two structures of the visual pathway. In accordance to the maps presented in Figure 7, negative BOLD responses are found in V1 at 10 Hz.

Additionally, BOLD responses in the SC and LGN reached their maximum amplitude at about 4 to 5

seconds after the onset of stimulation for all stimulus conditions, while responses in V1 required about 5 to 8 seconds to reach the peak, as exemplified in Figure 4 for one stimulus condition. A second peak after the end of the stimulation was also found in the SC at almost all stimulus conditions, and in some cases in the LGN and V1.

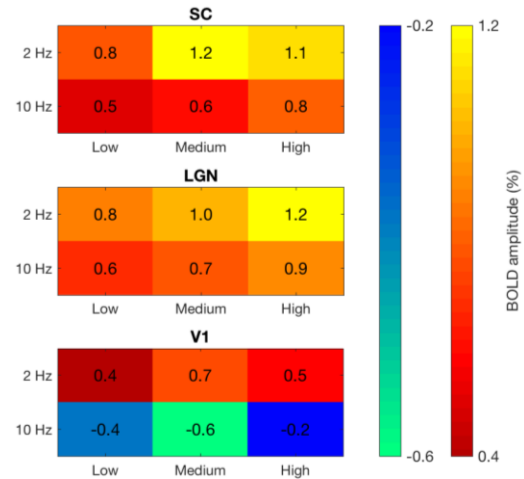


Figure 8 – Maximum BOLD percent signal change values in the SC, LGN and V1 for flickering stimuli at 2 Hz or 10 Hz and low ($9.2 \times 10^{-3} \text{ W/m}^2$), medium ($9.2 \times 10^{-2} \text{ W/m}^2$) or high ($8.1 \times 10^{-1} \text{ W/m}^2$) intensities.

Experiment 2: BOLD responses to different frequencies under etomidate

The etomidate anaesthetic regime produced a stable respiratory rate and temperature of 104 ± 20 breaths/min and $35.5 \pm 1.4 \text{ }^\circ\text{C}$ (values indicated as mean \pm standard deviation), respectively, in the 4 mice that were used in Experiment 2. Despite the physiological stability, one mouse of this experiment died within one day after the end of the session. This mouse also revealed almost no response to the stimuli in the visual pathway. Therefore, the data from this mouse was not included in the group analysis.

The group-level maps for each frequency are shown in Figure 9 for 2 Hz of flickering frequency, Figure 10 for 5 Hz, Figure 11 for 10 Hz and Figure 12 for 20 Hz stimuli. In general, significant BOLD responses to the stimuli are identified in the SC, V1 and LGN, but not at all frequencies. In particular, the SC responds to almost all flickering frequencies, registering high t -values in both sides of the brain, the highest being detected at 2 Hz. Furthermore, the span of the activation seems to be approximately equal for the 2 Hz, 5 Hz and 10 Hz frequencies. However, the group-level map for 20 Hz stimuli does not document significant SC responses. Clusters of activation in the LGN also seem to be approximately of the same size for the three lower frequencies of stimulation, and significantly reduced for the 20 Hz. On the other hand, the t -values in V1 show a clear negative trend with frequency, with the

highest t -values and number of responsive voxels being detected at 2 Hz, and the lowest t -values at 20 Hz. Although V1 responds to all frequencies, relatively few voxels are considered statistically significant at 5 Hz and 10 Hz.

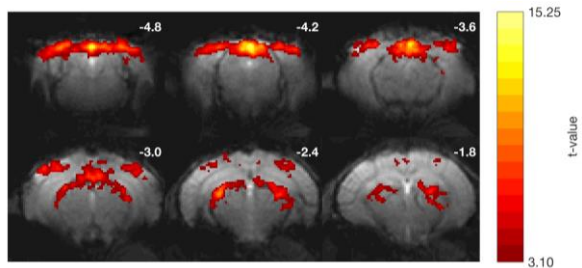


Figure 9 – Brain map of significant ($p < 0.001$, minimum cluster size = 8) BOLD activation to binocular visual stimulation with 2 Hz flashing frequency in consecutive coronal slices from an average of 3 mice ($n = 6$ runs). Approximate distances from Bregma are indicated in each slice.

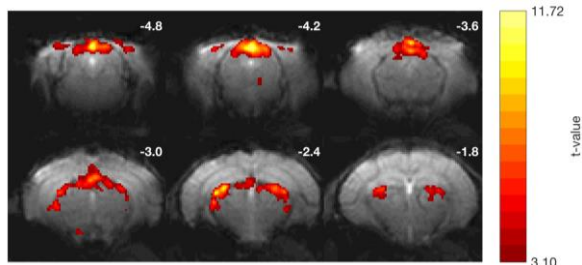


Figure 10 – Idem to Figure 11, but for 5 Hz.

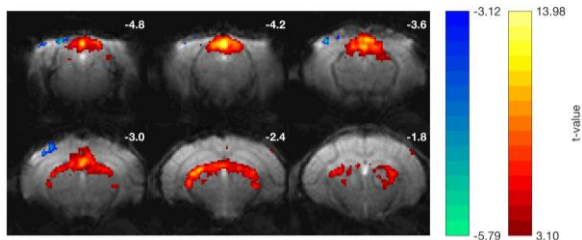


Figure 11 – Idem to Figure 11, but for 10 Hz.

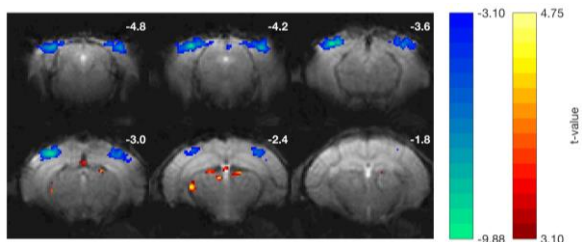


Figure 12 – Idem to Figure 11, but for 20 Hz.

As observed in Figure 13, the smallest peak amplitudes of the average cycle of the BOLD response in the SC and LGN were detected at 20 Hz. On the contrary, responses in these regions attained high peak values at the other tested frequencies, with LGN reaching the highest percent signal change values. Whereas responses in V1 at 2 Hz and 5 Hz are clearly positive in both sides of the brain, reaching their peaks at positive values, BOLD responses at 10 and 20 Hz exhibited negative peaks. A negative trend with frequency is found in the BOLD contrast of V1, with

the most negative peak value being registered for 20 Hz.

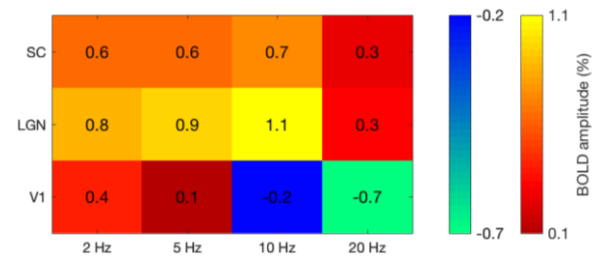


Figure 13 – Maximum BOLD percent signal change values in the SC, LGN and V1 for flickering stimuli at 2 Hz, 5 Hz, 10 Hz or 20 Hz.

Similar to what is shown for Experiment 1, responses in the SC and LGN reached their maximum amplitude at about 4 to 5 seconds after the onset of stimulation for 2 Hz, 5 Hz and 10 Hz stimuli. Moreover, responses in V1 at 2 Hz and 20 Hz reached the positive or negative peak at 6 and 8 seconds, respectively. However, times to peak in the SC and LGN at 20 Hz and in V1 at 5 Hz and 10 Hz deviated from these intervals. Responses in the SC and LGN peaked around 3 seconds at 20 Hz, while responses in V1 at 5 Hz and 10 Hz peaked (positively and negatively, respectively) after 4 and 9 s, respectively. Nevertheless, it should be noted that these responses do not have very well-defined peaks compared with the others, since variations from the baseline are very small.

Experiment 3: BOLD responses under medetomidine

The physiological parameters of all mice used in this experiment were stable during the entire experimental session, with a mean \pm standard deviation of 112 ± 16 breaths/min and 35.0 ± 1.2 °C across all mice. Moreover, due to the administration of atipamezole, medetomidine effects could be reversed and mice could return to their normal state within 15 minutes after injection of the antagonist. It should be noted, however, that the one mouse used in this experiment was found dead within one week after the experimental session. Nonetheless, in this case, one cannot infer if this was caused by the administration of medetomidine or by any other reason intrinsic or extrinsic to the experiment. It is also important to report that, on the contrary to mice anaesthetized with etomidate, these three mice started to move while they were still in the scanner, respectively 3 h, 1 h 50 min, and 2 h 50 min after the bolus of medetomidine.

According to the group visual map for 2 Hz stimuli shown in Figure 14, the greatest density of voxels with statistically significant responses is found in the SC, V1 and LGN. Moreover, this map showed higher t -values in comparison to the

equivalent maps obtained for mice sedated with etomidate presented in the bottom of Figure 6 and in Figure 9.

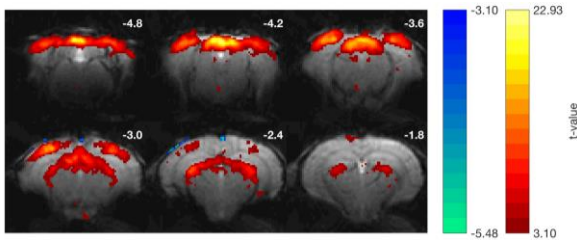


Figure 14 – Idem to Figure 11, but for medetomidine.

Mean BOLD responses to the visual stimulus for the LGN, SC and V1 are shown in Figure 15 for mice anaesthetized with medetomidine and mice anaesthetized with etomidate from Experiment 2.

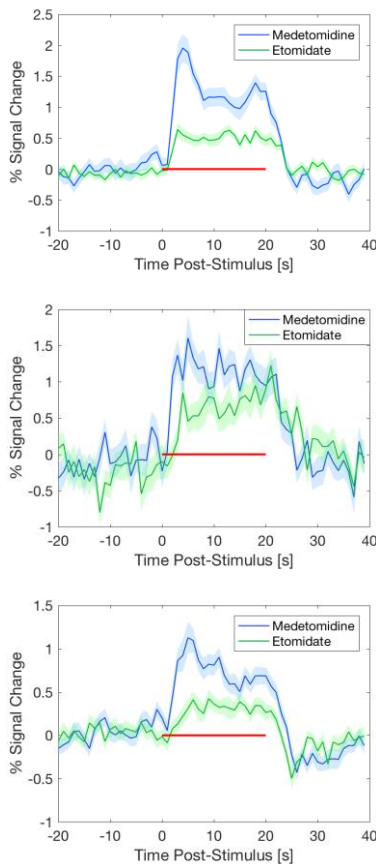


Figure 15 – Cycle of the BOLD response to binocular visual stimulation with 2 Hz flashing frequency in the SC (Top), LGN (Middle) and V1 (Bottom) of mice anaesthetized with medetomidine (blue tones) and etomidate (green tones). Timecourses were averaged over 3 animals ($n = 6$ runs) and plotted as mean percentage of signal change (solid line) \pm standard error of the mean (shaded region). The red bars indicate 20 s stimulation periods.

The maximum BOLD percent signal change value differs between each region of medetomidine-sedated mice, with the highest being found in the SC (approximately 2.0%) and the lowest in V1 (about 1.1%). Peak amplitude in the LGN is found at 1.6%. Moreover, these structures reach their maximum contrast about 4 to 5 seconds

from the stimulus onset. Additionally, the SC shows a strong decrease in the BOLD contrast after the initial peak, exhibiting a second peak in activation slightly before stimulation is turned off. Contrarily, LGN response appears to remain constant throughout the whole stimulation period. V1 response is also shown to slightly decrease throughout the entire period and to go below baseline for some seconds when stimulation is off.

3.2. Optimization of Etomidate Dosage

All mice that were subjected to different etomidate dosages remained stabilized and motionless during the 3 hours under etomidate sedation, with the exception of two mice in which isoflurane was discontinued too early (20 minutes after bolus), and that exhibited some movements \sim 3-7 minutes after isoflurane was lowered to 0%. Nevertheless, after introducing isoflurane at 0.5-1% for 10 more minutes, both these mice remained stable until the end of the experiment, without having any other burst of activity. In the end of the experiment, only one mouse died. This animal belonged to the group that was administered with the highest dosage of etomidate.

4. Discussion

4.1. Visual Stimulation fMRI Experiments

Light intensity and frequency tuning under etomidate. Regions exhibiting highly significant BOLD activation upon visual stimulation in all experiments performed in this project included the SC, LGN and V1, which is in agreement to previous rodent visual fMRI studies [14][19][23][24].

As observed in the maps shown in Figure 6 and Figure 7, the t -values and the number of responsive voxels in the SC increased from the lowest intensity ($9.2 \times 10^{-3} \text{ W/m}^2$) to the higher intensities ($9.2 \times 10^{-2} \text{ W/m}^2$ and $8.1 \times 10^{-1} \text{ W/m}^2$). Moreover, when analysing the dynamics of the response at the ROI level (Figure 8), smaller BOLD amplitudes were detected in the SC and LGN for the lowest intensity in comparison to the others, either for 2 Hz or 10 Hz flashing stimuli. These results are in good agreement with the results obtained by Zhang et al. [19], which found that BOLD response in the SC of Sprague-Dawley rats is weaker under dim light and that it saturates at higher intensities, suggesting that these dependences reflect retinal responses.

Maximum BOLD percent signal change values found in the SC, LGN and V1 for flickering stimuli at 2 Hz, 5 Hz and 10 Hz (Figure 13) are very close to the values found for the BOLD contrast in the fMRI study in mice done by Niranjana and colleagues [14]. In contrast to what they found, responses in the SC and LGN in the present work did not show a positive trend in BOLD am-

plitude with increasing frequency. Even if the amplitude of the BOLD response in Experiment 2 slightly increased from 2 Hz to 10 Hz stimuli for both of these regions, the same was not detected in Experiment 1 (Figure 8). Nevertheless, it should be noted that the slope of the increase of the BOLD contrast with frequency found in their study was not very steep either, and that the strongest frequency preference was found in V1 in comparison to those subcortical structures. Moreover, the bilateral negative BOLD responses elicited in V1 at 10 Hz (Figure 7 and Figure 11), and the negative trend it shows in response to increasing frequency are in agreement with their findings. They suggested that these negative responses observed at higher frequencies can be explained by a breakdown in neurovascular coupling at higher temporal frequencies, or by inhibitory neurons elsewhere in the brain that decrease neuronal activity in V1 and trigger these negative BOLD responses.

In this study, the temporal resolution was 1 second, rendering a proper separation of rise times infeasible. Nevertheless, after carefully visualizing the average cycles of the BOLD responses obtained with the study, it was possible to infer that the SC and the LGN peaked at about 4 to 5 seconds after stimulus onset, and the V1 at about 5 to 8 seconds. It is known that V1 receives visual information from the dorsal LGN through the optic radiation [25], which might explain this delay in the time-to-peak observed in V1 in comparison to the subcortical structures.

Comparison between etomidate and medetomidine

The present study has demonstrated that regions of the visual pathway that exhibit significant responses to binocular visual stimuli in mice anaesthetized with medetomidine (Figure 14) also show significant responses in mice anaesthetized with etomidate under the same stimulus conditions (Figure 6 and Figure 9). Besides that, results regarding the frequency tuning capability of the SC, LGN and V1 observed in this work are very similar to the ones obtained from mice anaesthetized with medetomidine [14], proving that subcutaneous etomidate is also a suitable anaesthetic for functional studies in mice.

Sedation with medetomidine did not last for more than 3 hours in either of the three mice of Experiment 3, which led to an uneven number of runs performed across mice. Although it was only necessary to run a few acquisitions in this particular study in order to be able to make direct comparisons between the two anaesthetic regimes, this premature motion of the animals can compromise the completeness of future more complex fMRI experiments that require longer

scanning sessions. Moreover, subcutaneous etomidate avoids the large infusion volumes and complex experimental setup that intravenous infusion requires for mice [17], decreasing the risk of fluid overload or pulmonary edema [16].

Despite these important advantages of subcutaneous etomidate, some relevant differences between these two anaesthetics (etomidate and medetomidine) are worth mentioning. First, three mice died after being subjected to etomidate sedation. Two of these mice exhibited lack of responsiveness of the visual centres being studied in comparison to the other mice, resulting in their discarding from the group analyses. Secondly, the group-level statistical parametric map obtained from mice anaesthetized with medetomidine (in Figure 14) revealed higher t -values in comparison to the equivalent maps obtained for mice sedated with etomidate (Figure 6 and Figure 9). Moreover, despite that the shape of the BOLD responses in the SC, LGN and V1 was similar for both anaesthetics, ROI analyses in those regions revealed higher maximum BOLD percent signal change values in mice anaesthetized with medetomidine, as it can be confirmed by comparing timecourses displayed in the ROI plots of Figure 15.

All this cumulative evidence points to the same conclusion: the protocol suggested by Klee et al. [17] may not be optimal for long fMRI scanning sessions, and may in fact be much too stringent. The possibility of decreasing the dosage of etomidate should be tested, such that the mortality rate and functional SNR of these experiments are matched or superior to medetomidine.

4.2. Optimization of Etomidate Dosage

We have attempted to decrease etomidate dosage and still maintain a sufficient depth of anaesthesia during the whole experiments. Our preliminary results show that mice can remain physiologically stable and motionless even if the constant infusion dosage is decreased to 1/3 of its initial value. Even more promising, it should be noted that the mice subjected to lower dosages did not die although n.b. that only 3 animals were tested. Future work will test this new regime in the context of an fMRI session, along with its associated acoustic noises, in order to properly conclude if this decrease in the dosage still guarantees a sufficient depth of anaesthesia in mice that prevents them from moving when they are being intensively stimulated.

4.3. Setup for Delivery of Complex Visual Stimuli

Limitations in space were a major challenge when designing the setup developed for presentation of spatially structures visual stimuli to mice.

Therefore, even if small adjustments on the current position of the screen can be done in the future and other screens be added to the current setup, there will not probably be much space for large modifications. Smaller adjustments in the piece that was 3-D printed for accurate positioning of the OLED in front of the eye throughout experiments can be done in order to provide more stability to it and a better fixing to the animal bed.

The use of the OLED display instead of multiple fibre-coupled LED sources revealed to be a much lower cost and versatile solution, given the small budget that was required to buy all components of the setup (Figure 1) and the capability to provide a vast variety of stimuli that would not be possible with a limited number of fibre-coupled LEDs. The electronic components that were connected to the screen are at a sufficient distance to not be interfered by induced currents from the scanner, as it was verified when the setup was brought to the scanner room and some preliminary tests were done.

Given the orientation and direction selectivity as well as the speed tuning capability that have been observed in V1, LGN and SC of the mouse [6][26][27], the setup was programmed to deliver bars moving at different speeds along the vertical and horizontal directions in order to provide comparative fMRI data to complement the existing literature (Figure 2). Even though the setup has not been tested with an *in vivo* experiment in order to check if mice are responding to the designed stimuli, modifications can be readily incorporated into the stimulator given the flexible software control that is available and the easiness to print small 3-D pieces in a matter of minutes.

5. Conclusions and Future Work

This thesis focused on the development and demonstration of the suitability of a new non-invasive free-breathing anaesthesia protocol based on subcutaneous injection of etomidate for fMRI studies in mice. The mouse visual pathway was mapped using high-resolution BOLD fMRI following binocular stimulation with flashing lights at 9.4T. Highly significant BOLD responses were observed in the SC, LGN and V1 of the mouse brain at both subject and group levels, and for all stimulus conditions. Mice remained physiologically stable and motionless for the entire scanning session, on the contrary to mice anaesthetized with the state-of-the-art fMRI anaesthesia (medetomidine). Together, these observations validate the use of subcutaneously administered etomidate for visual fMRI in mouse models. However, an increased mortality rate likely reflects that the dosages used here were too high; nevertheless, we have shown that mice receiving

1/3 of the previous dosage also remain stable and motionless for a long period of time (>3 h). Future studies will repeat some of the fMRI experiments here to find the optimal dosage where mouse stay stable for >3 h, retain the BOLD responses, and recover well from the experiments. Supplementation of diet with vitamin C should also be attempted, given its capability to inhibit adrenal suppression caused by etomidate [28]. In addition, we will perform additional orthogonal physiological stability measurements, such as partial pressure of carbon dioxide (pCO₂) and partial pressure of oxygen (pO₂), as well as blood pressure, to show that the protocol provides very stable physiological conditions over time.

We have also developed the OLED screen and showed that it is compatible with the magnet environment. To our knowledge, this is the first attempt at building a system for small rodent preclinical fMRI capable of delivering complex 2-D stimuli, which will allow to study, among others, motion, orientation, direction or even shape dependence in the entire pathway. The capabilities of the system can be extended in the future, given the flexibility and ease of programming a wide variety of stimuli, to incorporate more screens into the setup and to print any 3-D pieces that would help fixing the screen(s) at the desired positions. Comprehensive fMRI experiments to investigate the global brain activity arising from complex pattern presentation in the mouse will be done in the near future to fully validate this new visual stimulation system. In turn, this will pave the way not only for studying complex stimuli, but also for optogenetic or other types of manipulations that are highly feasible in mice.

Finally, it is worth noting that the existing dataset can benefit from further analyses, such as mapping of coherence, that would enable detecting phase differences between BOLD signals of the different visual centres, thereby avoiding the need to assume an HRF model. These, as well as other more stringent statistical tests comparing between anaesthesia conditions, will be performed in the near future.

References

- [1] N. J. Priebe and A. W. McGee, "Mouse vision as a gateway for understanding how experience shapes neural circuits," *Front. Neural Circuits*, vol. 8, p. 123, Oct. 2014.
- [2] L. Luo, E. M. Callaway, and K. Svoboda, "Genetic dissection of neural circuits.," *Neuron*, vol. 57, no. 5, pp. 634–60, Mar. 2008.
- [3] W. Platzer and W. (Werner). Kahle, *Color Atlas of Human Anatomy, Vol. 3: Nervous System and Sensory Organs*, 5th ed. Thieme, 2003.
- [4] N. J. Gandhi and H. A. Katnani, "Motor Functions of the Superior Colliculus," *Annu. Rev. Neurosci.*, vol. 34, no. 1, pp. 205–231, Jul. 2011.

- [5] S. M. King, "Escape-related behaviours in an unstable, elevated and exposed environment. II. Long-term sensitization after repetitive electrical stimulation of the rodent midbrain defence system.," *Behav. Brain Res.*, vol. 98, no. 1, pp. 127–42, Jan. 1999.
- [6] M. S. Grubb and I. D. Thompson, "Quantitative Characterization of Visual Response Properties in the Mouse Dorsal Lateral Geniculate Nucleus," *J. Neurophysiol.*, vol. 90, no. 6, pp. 3594–3607, Aug. 2003.
- [7] C. M. Niell and M. P. Stryker, "Highly Selective Receptive Fields in Mouse Visual Cortex," *J. Neurosci.*, vol. 28, no. 30, pp. 7520–7536, Jul. 2008.
- [8] L. Wang, R. Sarnaik, K. Rangarajan, X. Liu, and J. Cang, "Visual receptive field properties of neurons in the superficial superior colliculus of the mouse.," *J. Neurosci.*, vol. 30, no. 49, pp. 16573–84, Dec. 2010.
- [9] S. Ogawa, T. M. Lee, A. R. Kay, and D. W. Tank, "Brain magnetic resonance imaging with contrast dependent on blood oxygenation.," *Proc. Natl. Acad. Sci. U. S. A.*, vol. 87, no. 24, pp. 9868–72, Dec. 1990.
- [10] L. Stefanacci *et al.*, "fMRI of monkey visual cortex.," *Neuron*, vol. 20, no. 6, pp. 1051–7, Jun. 1998.
- [11] W. Chen, X. H. Zhu, T. Kato, P. Andersen, and K. Ugurbil, "Spatial and temporal differentiation of fMRI BOLD response in primary visual cortex of human brain during sustained visual simulation.," *Magn. Reson. Med.*, vol. 39, no. 4, pp. 520–7, Apr. 1998.
- [12] N. K. Logothetis, H. Guggenberger, S. Peled, and J. Pauls, "Functional imaging of the monkey brain," *Nat. Neurosci.*, vol. 2, no. 6, pp. 555–562, Jun. 1999.
- [13] C. J. Bailey, B. G. Sanganahalli, P. Herman, H. Blumenfeld, A. Gjedde, and F. Hyder, "Analysis of Time and Space Invariance of BOLD Responses in the Rat Visual System," *Cereb. Cortex*, vol. 23, no. 1, pp. 210–222, Jan. 2013.
- [14] A. Niranjana, I. N. Christie, S. G. Solomon, J. A. Wells, and M. F. Lythgoe, "fMRI mapping of the visual system in the mouse brain with interleaved snapshot GE-EPI," *Neuroimage*, vol. 139, pp. 337–345, Oct. 2016.
- [15] M. M. Petrinovic *et al.*, "A novel anesthesia regime enables neurofunctional studies and imaging genetics across mouse strains," *Sci. Rep.*, vol. 6, no. 1, p. 24523, Jul. 2016.
- [16] P. V. Turner, T. Brabb, C. Pekow, and M. A. Vasbinder, "Administration of substances to laboratory animals: routes of administration and factors to consider.," *J. Am. Assoc. Lab. Anim. Sci.*, vol. 50, no. 5, pp. 600–13, Sep. 2011.
- [17] R. Klee *et al.*, "Etomidate anaesthesia for fMRI in mice revisited: Subcutaneous administration facilitates experimental procedures.," in *Proceedings of the 25th Annual Meeting of ISMRM*, 2017, p. 5316.
- [18] J. M. Adamczak, T. D. Farr, J. U. Seehafer, D. Kalthoff, and M. Hoehn, "High field BOLD response to forepaw stimulation in the mouse," *Neuroimage*, vol. 51, no. 2, pp. 704–712, Jun. 2010.
- [19] J. W. Zhang *et al.*, "BOLD Response Dependence on the Stimulation Light Intensity in the Rat Superior Colliculus," in *Proceedings of the 19th Annual Meeting of ISMRM*, 2011, p. 3677.
- [20] C. A. Schneider, W. S. Rasband, and K. W. Eliceiri, "NIH Image to ImageJ: 25 years of image analysis," *Nat. Methods*, vol. 9, no. 7, pp. 671–675, Jun. 2012.
- [21] E. S. Lein *et al.*, "Genome-wide atlas of gene expression in the adult mouse brain," *Nature*, vol. 445, no. 7124, pp. 168–176, Jan. 2007.
- [22] K. B. J. Franklin and G. Paxinos, *Paxinos and Franklin's the Mouse Brain in Stereotaxic Coordinates*, 4th ed. Elsevier, 2013.
- [23] C. Lau, I. Y. Zhou, M. M. Cheung, K. C. Chan, and E. X. Wu, "BOLD Temporal Dynamics of Rat Superior Colliculus and Lateral Geniculate Nucleus following Short Duration Visual Stimulation," *PLoS One*, vol. 6, no. 4, p. e18914, Apr. 2011.
- [24] C. P. Pawela *et al.*, "Modeling of region-specific fMRI BOLD neurovascular response functions in rat brain reveals residual differences that correlate with the differences in regional evoked potentials," *Neuroimage*, vol. 41, no. 2, pp. 525–534, Jun. 2008.
- [25] L. Erskine and E. Herrera, "Connecting the retina to the brain.," *ASN Neuro*, vol. 6, no. 6, 2014.
- [26] U. C. Dräger, "Receptive fields of single cells and topography in mouse visual cortex," *J. Comp. Neurol.*, vol. 160, no. 3, pp. 269–289, Apr. 1975.
- [27] S. Inayat, J. Barchini, H. Chen, L. Feng, X. Liu, and J. Cang, "Neurons in the Most Superficial Lamina of the Mouse Superior Colliculus Are Highly Selective for Stimulus Direction," *J. Neurosci.*, vol. 35, no. 20, pp. 7992–8003, May 2015.
- [28] M. P. Boidin, W. E. Erdmann, and N. S. Faithfull, "The role of ascorbic acid in etomidate toxicity.," *Eur. J. Anaesthesiol.*, vol. 3, no. 5, pp. 417–22, Sep. 1986.